Synthesis of biobased superabsorbent hydrogel

Highlights

This chapter describes the synthesis, characterization, and property evaluation of starch, itaconic acid (IA) and acrylic acid (AA)-based superabsorbent hydrogels (SAHs). These hydrogels were prepared through free radical polymerization method using N,N'-methylene bis-acrylamide (MBA) as the cross-linker and ammonium persulfate (APS) as the initiator. Different compositions of SAHs were prepared and their performance was evaluated towards water absorption with and without load, and in salt solutions. Further, water swelling kinetic of the SAHs were studied using different kinetic models. Moreover, control urea release property and biodegradability of the prepared SAHs were also confirmed via fertilizer release and soil burial test, respectively. In addition, the effect of urea loaded SAHs on water holding capacity, soil porosity, and germination rate of okra seeds was also investigated.

Parts of this chapter are published as

[1] Bora, A. and Karak, N. Starch and itaconic acid-based superabsorbent hydrogels for agricultural application. *European Polymer Journal*, 176:111430, 2022.

2.1. Introduction

From **Chapter 1**, it is seen that superabsorbent hydrogel (SAH) has occupied a decent position in the scientific community over the last two-three decades. Their extraordinary network structure and significant water absorption capacity (WAC) make them suitable to be used in many fields including agriculture, personal hygiene, wound dressing, tissue engineering, drug delivery, waste-water treatment, etc. [1]. Recently, SAHs have attracted great attention as water absorption materials for agricultural applications in arid and semi-arid regions. Moreover, they are also used as slow-release fertilizer (SRF) system to supply nutrients to the plant in a controlled manner, leading to an increase in crop yield along with a reduction of fertilizer loss [2]. However, most of the SAHs are synthesized from synthetic polymers such as poly(acrylic acid) (PAA) [3], poly(acrylamide) (PAM) [4] or their copolymers which are obtained from non-renewable resources and are not environmentally friendly. Therefore, biobased SAHs are considered as advantageous than synthetic ones due to their easy availability, biocompatibility and biodegradability attributes [5]. They are mainly prepared from polysaccharides such as starch, cellulose, xanthan gum, alginate, chitosan, etc. and their polymeric backbones are grafted with vinyl monomers such as acrylonitrile (AN), methacrylic acid (MAA), acrylamide (AM), acrylic acid (AA), etc. to increase the hydrophilicity and swelling rate of the SAH [6]. However, there is still a significant amount of petroleum-based vinyl monomers are used which is posing serious threats to sustainability of the ecosystem unsuitable for agricultural applications [7]. In this vein, various biobased monomers including itaconic acid (IA), citric acid (CA), and lactic acid (LA) have been intensively studied for fabrication of biobased SAHs [8-10]. Lots of literature are available on the synthesis of biobased hydrogels which were chemically modified to improve their biocompatibility, biodegradability, and to reduce toxicity [11]. Therefore, in this chapter, it is aimed to increase the total amount of biobased components on the starch-based SAH by amalgamating IA as compared to the previously reported SAHs. For this purpose, four different SAHs with different biobased components (48-63%) were synthesized using the solution polymerization method and their swelling capacity in different liquid media was studied. In addition to these, water absorption under load (AUL), swelling kinetic studies, fertilizer release rate, biodegradability, soil water holding capacity (WHC), porosity and germination rate of

okra seeds of the prepared SAHs were also investigated to study their potential ability for using in agricultural applications.

2.2. Experimental section

2.2.1. Materials

Starch **(Table 1.1, Chapter 1)** and AA **(Table 1.2, Chapter 1)** were obtained from Hindustan Gum & Chemicals Ltd (Bhiwani, India). Starch is isolated from corn in white powder form. It is insoluble in water, but soluble when heated to about 80-90 °C and it is used as the main biobased raw material to prepare hydrogels. AA is used as the monomer to prepare hydrogels. The molecular weight of AA is 72.06 g/mol and its density is 1.05 g/cm^3. It was used without being further modified.

IA **(Table 1.2, Chapter 1)** is a dicarboxylic acid, used as biobased monomer to increase the bio-content in the prepared hydrogel. It has a molecular weight of 130.10 g/mol and it was supplied by Sigma-Aldrich, Germany.

N,N'-methylene bis-acrylamide (MBA) **(Figure 1.1, Chapter 1)** as a cross-linker was used to prepare the hydrogel. It has a molecular weight of 154.17 g/mol and was obtained from SRL, India.

Ammonium persulfate (APS) is an inorganic salt, used as an initiator to fabricate the hydrogels. It is soluble in water and thermally dissociates to form anionic radicals. It has a molecular weight of 228.18 g/mol.

Sodium hydroxide (NaOH) solution was used as a neutralizing agent. NaOH was obtained from SRL, India.

Sodium chloride (NaCl) was used as a testing medium to investigate the effect of salt on WAC of the hydrogels. It was procured from Merck, India.

Methanol (CH_3OH) was used to wash hydrogel. It is supplied by Merck, India.

Urea was used as a nitrogen fertilizer to investigate the slow-release of fertilizer. It is soluble in water, and it has a molecular weight of 60.02 g/mol. It was purchased from Merck, India.

4-(Dimethylamino)benzaldehyde (DMAB) is a coloring reagent used to analyze urea content in fertilizer release tests. It was purchased from Merck, India. Its molecular weight is 149.19 g/mol.

Okra seeds were purchased from local markets in Sonitpur, Assam, India for seed germination test.

2.2.2. Methods

2.2.2.1. Synthesis of SAHs

SAHs were prepared by grafting AA and IA on the starch backbone in the presence of APS and MBA as the initiator and cross-linker, respectively using a solution polymerization technique [12]. To evaluate the effect of IA to AA ratio (IA: AA), SAHs with different compositions of AA and IA were prepared by keeping the amount of starch, MBA and APS fixed at 1 g, 0.5% and 2% (relative to the total amount of starch, AA and IA), respectively. Initially, starch and IA were added into 10 mL of NaOH solution (0.067 N) in a 250 mL three-neck round bottom flask which was equipped with a mechanical stirrer and a nitrogen inlet. The mixture was continuously stirred and heated slowly up to 85±5 °C. When the temperature reached 60 °C, AA with 1 mL of distilled water was added into the reaction mixture and stirred until starch turned into a gelatinized texture. After 20 min, the temperature of the reaction was reduced to 50 °C, followed by the addition of MBA and APS in 1 mL of distilled water into the reaction mixture. Thereafter, the reaction was allowed to polymerize under the nitrogen environment and the temperature was raised again up to 75±5 °C. When the product started to form, a definite volume of NaOH (8 N) was added to neutralize the remaining -COOH group present in the polymeric chains. After completion of the reaction, the solid material so obtained was allowed to swell in distilled water for 24 h. Swollen SAHs were filtered and washed with methanol, followed by drying in a hot air oven at 60 °C. Finally, dried SAHs were ground into a fine powder and used for further studies. As prepared SAHs containing biocomponents of 48%, 53%, 58% and 63% were labelled as H-1, H-2, H-3, and H-4, respectively. Different amounts of components used in the synthesis of the SAHs are presented in **Table 2.1.**

Table 2.1. Compositions of prepared SAHs.

Hydrogel	Starch (g)	AA (g)	IA (g)	MBA (%)	APS (%)
H-1	1	1.050	0	0.5	2
H-2	1	0.945	0.1	0.5	2
H-3	1	0.840	0.2	0.5	2
H-4	1	0.735	0.3	0.5	2

2.2.2.2. Synthesis of urea encapsulated SAHs (USAH)

USAH were prepared via the *in-situ* loading method following the same procedure as described in the previous section. Additionally, urea (1 g) was added to the starch and IA mixture in the first step followed by the addition of other components (AA, cross-linker, and initiator). After neutralization with 8 N NaOH solution, it was washed with distilled water and dried in an oven to study the urea loading as well as release behavior of the USAHs. Urea loaded H-1, H-2, H-3 and H-4 were labelled as UH-1, UH-2, UH-3 and UH-4, respectively.

2.2.2.3. Structural analysis

The FTIR spectra of synthesized SAHs were recorded on a Nicolet spectrophotometer (Impact-410 model, USA) by using potassium bromide pellets within the frequency range of 4000-400 cm^{-1}. The surface morphology of SAHs was studied by using scanning electron microscope (SEM) (JEOL, Japan, JSM 6390LV model). The thermogravimetric analyses (TGA) of prepared SAHs were performed using a TGA-4000 (PerkinElmer, USA) under inert nitrogen atmosphere from 30 to 600 °C with heating rate of 5 °C/min. Thermo Scientific (Evolution 300) UV-Visible spectrophotometer was used to measure the released urea content.

2.2.2.4. Swelling studies

In order to determine the maximum water swelling capacity (Q_{max}) of synthesized SAHs, the gravimetric method was used. A definite amount of finely powdered SAH was submerged in an excess amount of water until no more change in weight of the SAH was observed. It was eventually filtered to remove unabsorbed water from swollen hydrogel by using a stainless-steel sieve and the weight of the water absorbed hydrogel was correspondingly measured. The Q_{max} value was determined by using the following equation [13].

$$Q_{max} = \frac{W_1 - W_0}{W_0} \text{ ----------(Eq. 2.1)}$$

where W_o and W_1 are the weights of the SAH before and after swelling, respectively.

Moreover, the swelling capacity of SAHs in salt solutions were also determined by considering the concentration levels of salt. The swelling test was further carried out consecutively three times for each SAH to obtain the results accurately and the values were expressed as a mean of three replicates ± standard deviation.

2.2.2.5. Determination of percentage of grafting cross-linking and grafting cross-linking efficiency

The grafting parameters such as percentage of grafting cross-linking (GC%) and grafting cross-linking efficiency (GCE%) are the terms used to determine the percentage mass increased of the final product relative to the initial mass of the substrate [14]. In order to determine the percentage of GC and GCE, SAH products were washed with distilled water and dried in a hot air oven at 70 °C. Finally, dried SAHs were ground into powder and weight was measured. The following two equations are used to calculate GC (%) and GCE (%), respectively [12].

$$GC\ (\%) = \frac{(wt.\ of\ graft\ crosslinked\ hydrogel - wt.\ of\ CS)}{(wt.\ of\ CS)} \times 100 \text{ --------(Eq. 2.2)}$$

$$GCE\ (\%) = \frac{(wt.\ of\ graft\ crosslinked\ hydrogel - wt.\ of\ CS)}{(wt.\ of\ AA + IA)} \times 100 \text{ ------(Eq. 2.3)}$$

2.2.2.6. Determination of IA and AA content in the SAHs

The acid–base titration method is considered as a sensitive and simple way to determine the quantity of carboxylic acid groups present in the copolymer composition [12]. Since both IA and AA contain -COOH groups and they are present in prepared SAHs, so it is difficult to separately determine the amount of IA present in the SAHs. Therefore, the quantity of grafted IA and AA was determined by means of acid-base titration of carboxylic acid groups present in the unreacted material extracted from the SAH using Soxhlet extraction. Initially, hydrogels were dried in a hot air oven at 50 °C to a constant weight and a definite amount of dried hydrogel was subject to Soxhlet extraction. Based on the solubility of the IA and AA, previously weighed hydrogel was extracted with 200 mL of refluxed THF solvent for 3 h. After extraction, solvent was released in rotary evaporator and any remaining traces were removed by placing the flask in an oven at 70 °C for a certain time interval. Thereafter, unreacted material was dissolved in 15 mL of standard hydrochloric acid (0.1 N HCl) to completely protonate the carboxylate groups. The excess of HCl was titrated with standard NaOH solution (0.1 N) until pink color of the phenolphthalein indicator was observed. Then, the amount of acidic monomer units was calculated from the amount of NaOH required to deprotonate the -COOH groups.

2.2.2.7. Evaluation of water AUL

For determination of water AUL, a definite amount of SAH was placed in an empty tea bag and kept it in a 1000 mL beaker [1]. Then, a specific amount of load (500 g) was applied on top of the tea bag followed by pouring water or the solution into the beaker, slowly. After soaking for 5 h, the swollen bag was taken out of the beaker and the weight of the swollen SAHs was measured. In this work, the test was carried out in distilled water as well as in 0.05% NaCl solution. The AUL was calculated based on the equation as given below [15].

$$\text{AUL} = \frac{W_1 - W_0}{W_0} \text{ ----------(Eq. 2.4)}$$

where W_0 and W_1 are the weights before and after applying load on the SAHs, respectively.

2.2.2.8. Kinetic studies for swelling

Investigation of swelling kinetics was performed towards water absorption rate and water swelling capacity of the hydrogels, as both are important for agricultural applications [16]. To carry out the investigation, a predetermined amount of SAH was immersed in an excess amount of distilled water for different time durations (10, 20, 30, 40, 50, 60, 90, 120, and 240 min). After the specified period, swollen SAH was filtered by using a stainless-steel sieve to remove unabsorbed water. Then, the weight of the water absorbed SAH was measured and its water swelling capacity at a particular time interval was determined using **Eq. 2.1.** [17].

From these results, the water diffusion mechanism of the SAHs was observed by using the following equation.

$$\frac{W_t}{W_{eq}} = k t^n \text{ ----------(Eq. 2.5)}$$

$$\log\left(\frac{W_t}{W_{eq}}\right) = \log(k) + n\log(t) \text{ ----------(Eq. 2.6)}$$

where W_t and W_{eq} are the amount of water uptake at time (t) and equilibrium swelling i.e., maximum swelling capacity of the SAH, respectively. The proportionality constant (k) is related to the structure of hydrogel, while the diffusional exponent (n) illustrates the type of diffusion mechanism. The values of n and k were obtained from the slope and the intercept of the straight line by plotting the graph $\log(W_t/W_{eq})$ versus log(t). The obtained n values further corresponded to different diffusion mechanisms. The Fickian diffusion mechanism is followed when n value is less than 0.5, in which water diffuses

simply through the pores of SAH, wherein the mechanism is considered as non-Fickian diffusion when n value ranges between 0.5 and 1. In this case, two processes occurred simultaneously, i.e., diffusion of water through the pores of the polymer network as well as macromolecular relaxation of the polymer chain. Finely, for n values more than 1, diffusion is mainly governed by macromolecular relaxation [18,19].

Moreover, the experimental swelling results were further used to study the swelling kinetics of the 'as prepared' SAHs by using the following pseudo-second-order (PSO) kinetic equation.

$$\frac{t}{W_t} = \frac{1}{k_s W_{eq}^2} + \frac{t}{W_{eq}} \text{ ----------(Eq. 2.7)}$$

where W_t is the swelling value at time t, W_{eq} is the theoretical equilibrium swelling value and k_s is the swelling rate constant. From the plot of t/W_t against t, these kinetic parameters were obtained as slope and intercept of the straight line [20].

2.2.2.9. Urea loading and release studies

In order to determine the amount of urea loaded and released by SAHs, a previously reported method was followed [21,22]. Briefly, 1800 µL of Ehrlich's reagent (20 mmol/L DMAB dissolved in methanol) was protonated with 67 µL of hydrochloric acid (37 wt%) to generate electron-deficient carbonyl carbon, which upon further reaction with urea solution (1000 µL), a greenish yellow color complex was formed. The general reaction for the formation of the complex is shown in **Scheme 2.1**. The absorption of the visible light by the complex was measured at 420-430 nm wavelength. Thereby, a standard curve (concentration against absorbance) was plotted by measuring absorbance values for six different known concentrations of urea solutions (0.25, 0.125, 0.062, 0.031, 0.016, and 0.008 M) using a UV-visible spectrophotometer. From the plot, an equation of a straight line was obtained as given below.

$$y = 9.7663x + 0.0577 \text{ ----------(Eq. 2.8)}$$

where y and x are absorbance and concentration of the urea solution, respectively. The constant 9.7663 and 0.0577 are the slope and intercept of the straight line, respectively. By putting the value of absorbance into the **Eq. 2.8**, concentration of urea for unknown solution was determined.

In order to determine the loading percentage of urea, USAH was washed with 100 mL of distilled water after the completion of the reaction. Then, 1 mL of the solution was taken

out and absorbance was recorded using the UV-visible spectrophotometer according to the method as described above. From the absorbance value, the concentration of washed-out urea was determined. The percentage of urea loading efficiency was calculated by using the following equation.

$$\text{Urea loading efficiency (\%)} = \left(\frac{W_i - W_{wo}}{W_i}\right) \times 100 \text{ ----------(Eq. 2.9)}$$

where W_i is the amount of initially loaded urea and W_{wo} is the amount of washed-out urea. The urea loading study was performed three times for each sample and their mean values were utilized.

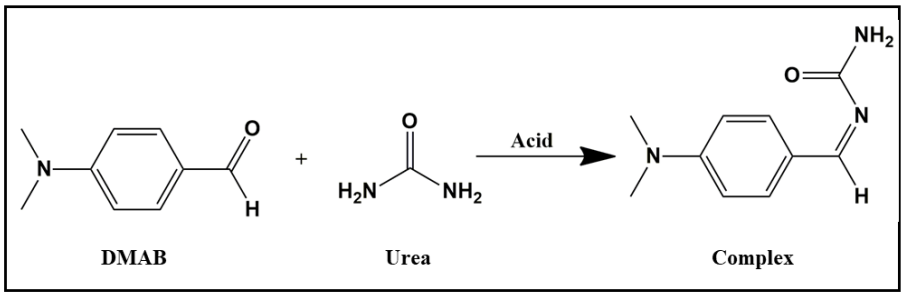

Scheme 2.1. General reaction for formation of the greenish yellow complex.

Likewise, urea release behaviors of the synthesized USAHs were studied. In this regard, dried USAH was put in an empty tea bag and immersed in a beaker containing 100 mL of distilled water. After immersion for a certain period time (1, 5, 15, 20 and 30 days), 2 mL of solution was taken out for determination of released urea contents. Immediately, 2 mL of distilled water was added to the beaker to keep the volume of the solution constant. Then, the concentration of urea released was determined by using **Eq. 2.8**. The percentage of urea released was obtained by using the following equation [13].

$$\text{Urea release (\%)} = \frac{M_t}{M_1} \times 100 \text{ ----------(Eq. 2.10)}$$

where M_1 is the remaining amount of loaded urea after washing of USAHs and M_t is the amount of urea released at time t. The urea release study was performed for each sample and the results were utilized for plotting the data.

2.2.2.10. Biodegradation study

2.2.2.10.1. Soil burial test

To study the biodegradation of the prepared SAHs, the soil burial test was performed with a slight modification of the method as described by Dutta *et al.* [23]. Initially, the

elemental compositions of the soil (carbon: 3.25 wt%, hydrogen: 0.4 wt% and nitrogen: 0 wt%) were determined using a CHN analyzer. In addition, pH of the collected soil was found to be slightly alkaline in nature (pH = 8.52). Furthermore, collected soil was separated from the foreign particles using a stainless-steel sieve. A definite amount of SAH was put in a tea bag and placed inside a paper cup with soil. Six sets of samples for each SAH were prepared in this way. Before burying the samples, water was added to each cup to make the soil pasty and then buried under garden soil at 6-10 cm depth. The test was carried out for 45 days and water was sprayed every alternate day to keep the soil moisture level constant. The samples were taken out one by one at a certain time interval (15, 30 and 45 days) for testing their biodegradation. The bag containing the sample was cleaned properly with distilled water and dried in a hot air oven at 50°C until a constant weight was obtained. The weight of the dried samples was measured and percent weight loss was calculated by using the following equation [13].

$$\text{Weight loss (\%)} = \left(\frac{W_i - W_f}{W_i}\right) \times 100 \text{ ----------(Eq. 2.11)}$$

where W_i and W_f are the initial and final weights of the sample before and after biodegradation test.

2.2.2.11. Determination of WHC of the soil

To evaluate the effect of prepared SAHs as a soil conditioner, the WHC of treated soil was evaluated. The test was carried out using soil samples treated with UH-1, UH-2, UH-3 and UH-4. Moreover, a sample without USAH was taken as a control for comparison purposes. Initially, samples were prepared by mixing 20 g of air-dried soil with 0.04 g of USAH in a paper cup having small holes at the bottom. Then, 30 mL of tap water was added to each cup allowing the samples to absorb water up to their swelling capacity. After 3 days, the weight of each sample was measured to determine the increased WHC of the soil and it was calculated by using the following equation [24].

$$\text{WHC (\%)} = \frac{W_t - W_i}{W_i} \times 100 \text{ ----------(Eq. 2.12)}$$

where W_i is the initial weight of the sample before the addition of water and W_t is the weight of the sample after 3 days.

2.2.2.12. Determination of particle density (PD), bulk density (BD) and porosity of the soil

PD of soil was determined by following a standard method [25]. Firstly, the weight of an empty pycnometer was measured. Then, it was filled with air-dried soil (10 g) and the weight was measured again. Thereafter, it was filled with water and the total weight of the pycnometer containing soil and water, was determined. Finally, the pycnometer was filled with only water and weight was measured and PD of the soil was calculated by using the following equation.

$$PD = \frac{d_W(W_s - W_a)}{(W_S - W_a) - (W_{SW} - W_w)} \text{ ----------(Eq. 2.13)}$$

where d_w is the density of water, W_s is the weight of pycnometer including dry soil sample, W_a is the weight of empty pycnometer, W_{sw} is the weight of pycnometer filled with soil and water, and W_w is the weight of pycnometer filled with water only.

BD of soil treated with USAH was determined from modification of the method described by Thombare *et al.* [26]. For this, samples were prepared by mixing 0.04 g of USAH with 20 g of air-dried soil and taken in a paper cup having small holes at the bottom. The test was carried out in five different samples i.e., soil treated with (1) UH-1, (2) UH-2, (3) UH-3, (4) UH-4 and (5) soil without any treatment (control). After preparation of the samples, 30 mL of tap water was added to each cup, and they were kept at room temperature for 3 days. The air-dried soil was further dried in an oven and was sieved with stainless-steel sieve. Finally, BD was determined from the mass and volume of the soil [27,28].

$$BD = \frac{M}{V} \text{ ----------(Eq. 2.14)}$$

where M is the mass of dry soil and V is the total volume of soil.

Further, the porosity of the soil was calculated based on the values of PD and BD by using the following equation [26].

$$\text{Porosity (\%)} = \left[1 - \left(\frac{BD}{PD}\right)\right] \times 100 \text{ ----------(Eq. 2.15)}$$

2.2.2.13. Seed germination test

The seed germination test was carried out to study the effect of USAHs on the germination rate of ladies-finger (okra seeds, *Abelmoschus esculentus*). For this purpose, 0.15 g of USAH was mixed with 60 g of loam soil in a paper cup with small holes at the bottom. The experiment was carried out in six different culture media, (1) UH-1, (2) UH-2, (3) UH-3, (4) UH-4, (5) control-1 (soil containing hydrogel without urea) and (6)

control-2 (only soil). For each medium, nine okra seeds were buried (1-2 cm away from the surface) in three separate paper cups. The test was performed under laboratory conditions. Under this condition, the soil was irrigated with water at the beginning (i.e., before sowing of the seeds) and no water was added until the last day of the observation. After 7 days, germination rate for the seedlings was observed and the results were finally compared with the control [13].

The germination percentage of the seeds was determined when the growth length of the radicle was found to be 1-2 mm and it was calculated by using the following equation [29].

$$\text{Seed germination (\%)} = \frac{G}{T} \times 100 \text{ ----------(Eq. 2.16)}$$

where G is the number of seeds germinated and T is the total number of seeds tested for each culture medium.

2.3. Results and discussion

2.3.1. Synthesis of SAHs

The synthesis of SAHs was performed by a conventional free radical polymerization process using CS, IA and AA as the monomers with APS as the unimolecular initiator and MBA as the cross-linker. A facile solution technique was employed with water as the medium for the preparation of SAHs. The reaction scheme with the proposed mechanism for the formation of hydrogel is shown in **Scheme 2.2.**

SAHs were formed via a three-step process. The first step was the initiation step, where the sulphate anion radicals were produced by the thermal dissociation of APS, subsequently abstracting the hydrogen from the hydroxyl group of starch to generate macroradicals. The second step was the chain propagation step, where the macroradicals initiated the grafting copolymerization via donation of the radicals to the nearby AA and IA monomers subsequently the grafted chains were coupled with the end of the vinyl group of MBA to form the 3D cross-linked network structure. In the last termination step, two living polymeric chains obtained from chain propagation either undergo deprotonation or combine to terminate the grafting polymerization [19,20]. The total solid content and bicomponent content in each of these synthesized hydrogels are provided in **Table 2.2**. The percentages of total biocomponent of the SAHs were calculated by using **Eq. 2.17**. As an example, H-2 contains 53.53% of total biocomponents where the amount of starch, AA, IA and MBA were 1 g, 0.945 g, 0.1 g

and 0.01 g, respectively. Introducing these values in **Eq. 2.17**, we obtained the percentage of total biocomponent for H-2. From this table it is clear that these hydrogels contain high amounts of biobased moieties with renewability characteristics.

$$\text{Total biocomponents (\%)} = \left(\frac{wt.\ of\ starch + wt.\ of\ IA}{wt.\ of\ (starch + IA + AA + MBA)}\right) \times 100 \quad \textbf{--(Eq. 2.17)}$$

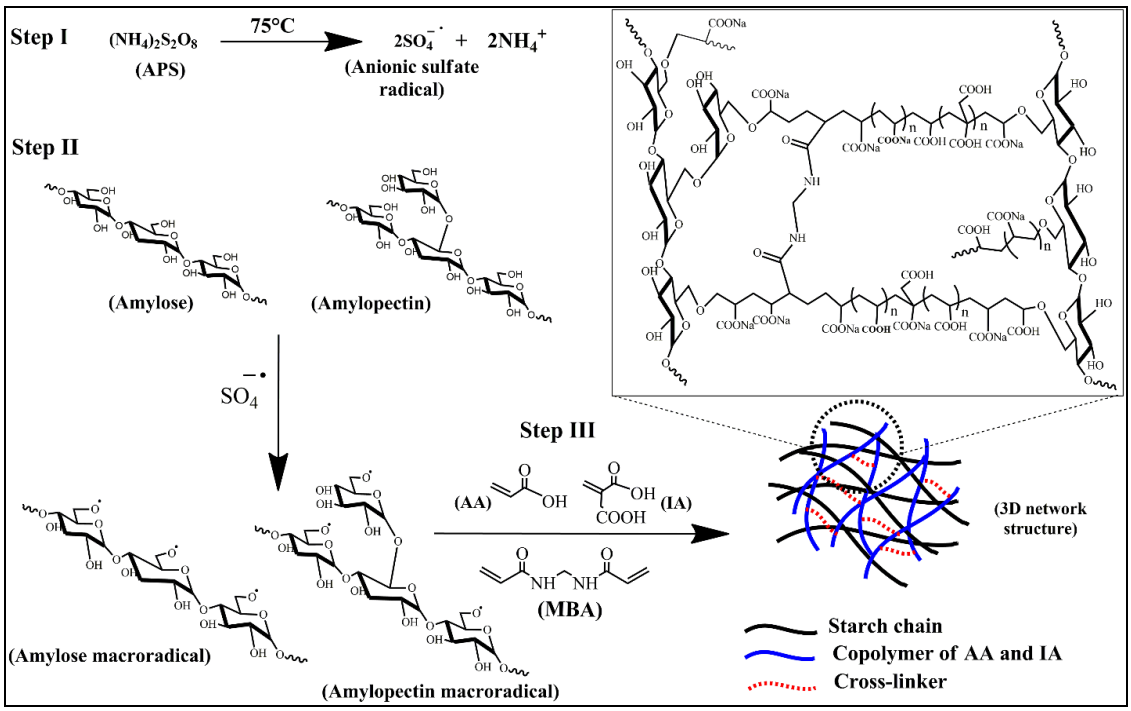

Scheme 2.2. Proposed reaction mechanism for synthesis of superabsorbent hydrogels.

Table 2.2. Details of percentage of GC, GCE, solid content and total biocomponent of hydrogels.

Hydrogel	GC (%)	GCE (%)	Solid content (%)	Total biocomponent (%)
H-1	146	139	17.17	48.54
H-2	134	128	17.12	53.53
H-3	121	117	17.37	58.54
H-4	112	109	17.48	63.57

2.3.2. Structural analysis

2.3.2.1. FTIR studies

FTIR spectral study was performed to investigate the grafting of AA and IA on the starch backbone and the obtained FTIR spectra for the synthesized SAHs are shown in **Figure**

2.1. A characteristic broad absorption peak centered at 3442 cm^{-1} was seen in FTIR spectra and attributed to the stretching vibration of O-H groups present in starch, AA and IA. The peaks that appeared at 2923 cm^{-1} and 2849 cm^{-1} correspond to an asymmetric and symmetric stretching frequency of CH_2 groups present in AA and IA in hydrogel structure [26]. The peak around 1720 cm^{-1} corresponds to the C=O stretching vibration of COOH groups which in turn overlaps with the band at 1647 cm^{-1} representing to N-H bending vibration, with a broad peak [26,30]. Further, peaks that appeared at 1447 cm^{-1} and 1410 cm^{-1} are assigned to symmetric stretching of COO^- groups and the peak around 1016 cm^{-1} is represents the ether linkage (C-O-C) present in the starch moiety [31]. From these characteristic peaks, it can be assumed that MBA, AA, and IA are grafted on the starch backbone and these moieties were involved in the formation of hydrogel structure.

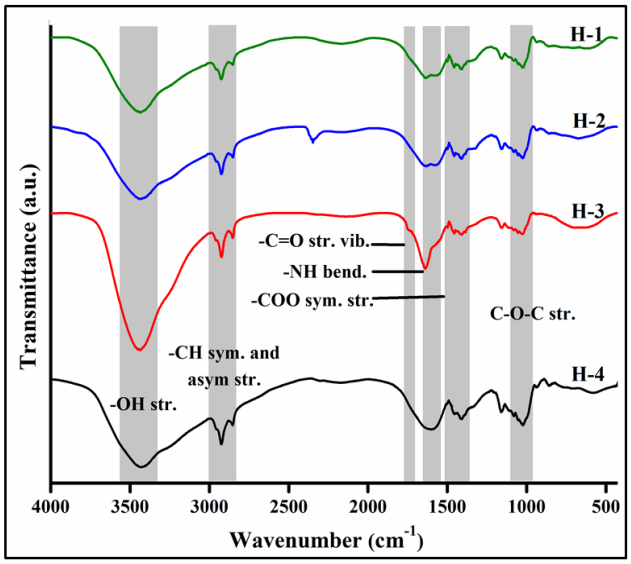

Figure 2.1. FTIR spectra of H-1, H-2, H-3 and H-4 hydrogels.

2.3.2.2. SEM analysis

To investigate the microscopic morphology of H-1, H-2, H-3 and H-4 hydrogels, SEM images (at 2000X magnification) were obtained, as shown in **Figure 2.2**. The porous network structure of all the hydrogels was observed in these images, which supports the formation of the 3D cross-linked network structure with the high-water absorption ability of the SAHs. Further, internally connected large pores were observed for these SAHs which are essential for the transportation of water and nutrient molecules in agricultural applications. However, the SEM image of the SAHs showed surface morphology and displayed pores with rough surface. It may be noted that the surface morphology of H-3 showed a little dense network structure as compared to other SAHs.

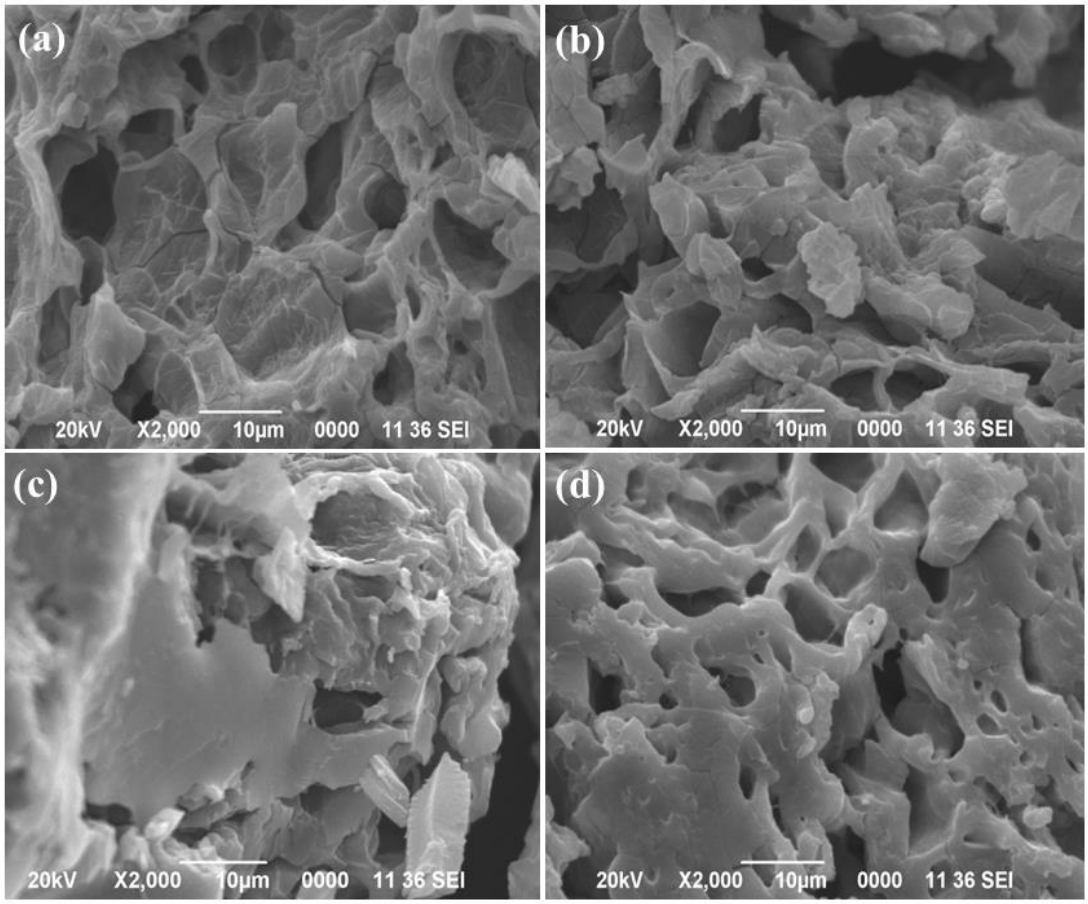

Figure 2.2. SEM images of hydrogel (a) H-1, (b) H-2, (c) H-3 and (d) H-4.

2.3.2.3. TGA analysis

In order to observe the effect of change in IA to AA ratio on the thermal stability of the prepared SAHs, thermal studies were performed. The TGA thermograms and first derivative of them are shown in **Figure 2.3**. The weight loss process for all the SAHs was found to occur in three well-differentiated degradation steps. Initially, the first step of degradation was observed up to 252 ℃ due to the loss of entrapped moisture present in the SAHs [13]. The second step of degradation for H-1, H-2, H-3 and H-4 were observed at 285 °C (29%), 298 °C (30%), 290 °C (27%), and 292 °C (34%), respectively and this step can be assigned to the degradation of main polymeric backbone [26]. Also, the third step of degradation can be ascribed to the breaking down of bonds between the polymeric backbone and grafting monomer and cross-linker present in the hydrogel network [26]. After this step, the remaining weight for H-1, H-2, H-3 and H-4 was 42%, 40%, 41% and 41%, respectively at 600 °C. From these results, it is observed that all the prepared SAHs exhibited almost similar thermal degradation characteristics, as their structures are alike.

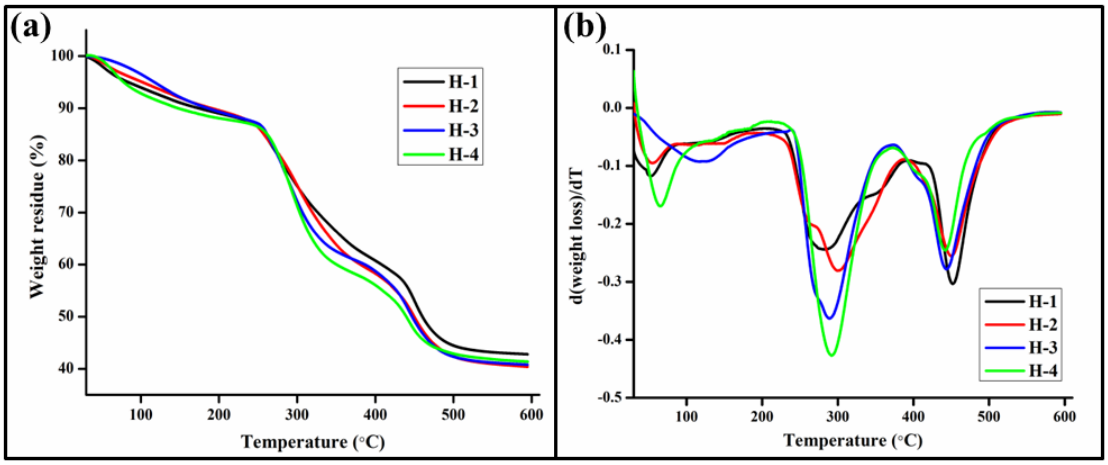

Figure 2.3. (a) TGA thermograms and (b) first derivative of TGA of SAHs.

2.3.2.4. Study of water absorption behavior of the SAHs in different media

The variation of water swelling capacity of H-1, H-2, H-3 and H-4 hydrogels in different media (distilled water and salt solution) is represented in **Figure 2.4.a**. It was found that H-1 was the highest swollen SAH (650±15 g/g), while H-4 was the least swollen SAH (154±8 g/g) according to their Q_{max} value in water. The Q_{max} value of SAHs was found to be decreased with the increase in the amount of IA in the compositions. This behavior was observed in the case of all three media. The Q_{max} values of the hydrogels were analyzed under the definite solid content and biocomponent content of the hydrogels as provided in **Table 2.2**. From this table, it is observed that the swelling results are consistent with the percentage of GC.

The percentage of GC decreases with the increase in the amount of IA in the SAHs which results in low swelling values. This can be attributed to the increase in the concentration of IA that increases the hydrophobic nature of SAHs due to the presence of unionized carboxylic acid groups in the polymeric chain which can lead to the decrease in swelling values of SAHs [32]. However, the water retention percentage of SAHs was found to be increased with an increase in the amount of IA in the SAHs, as shown in **Figure 2.4.b.** Percentage of water retention for H-1, H-2, H-3 and H-4 in salt solution (0.05% NaCl) was found to be as 30%, 35%, 33%, and 38%, respectively. This behavior can be attributed to the formation of a more compact structure as a result of the shielding effect of the cationic part of sodium chloride on the carboxylate group of IA and AA reducing the electrostatic repulsion in the hydrogel network structure which prevents the release of water molecules from the hydrogel network. A similar result was reported by Salimi *et. al.* in the case of the release of urea molecules by SRF formulation [31]. So, it can be

concluded that more water molecules can be retained by the SAHs containing more IA in saline solution. However, an unexpectedly lower retention capacity was observed in the case of H-3. In this case, a higher degree of neutralization can be suggested to be more effective than the salt effect. An increase in the degree of neutralization results in further increasing the ionic repulsion as well as hydrophilicity feature inside the polymer network that make permeation of water molecules easy [15].

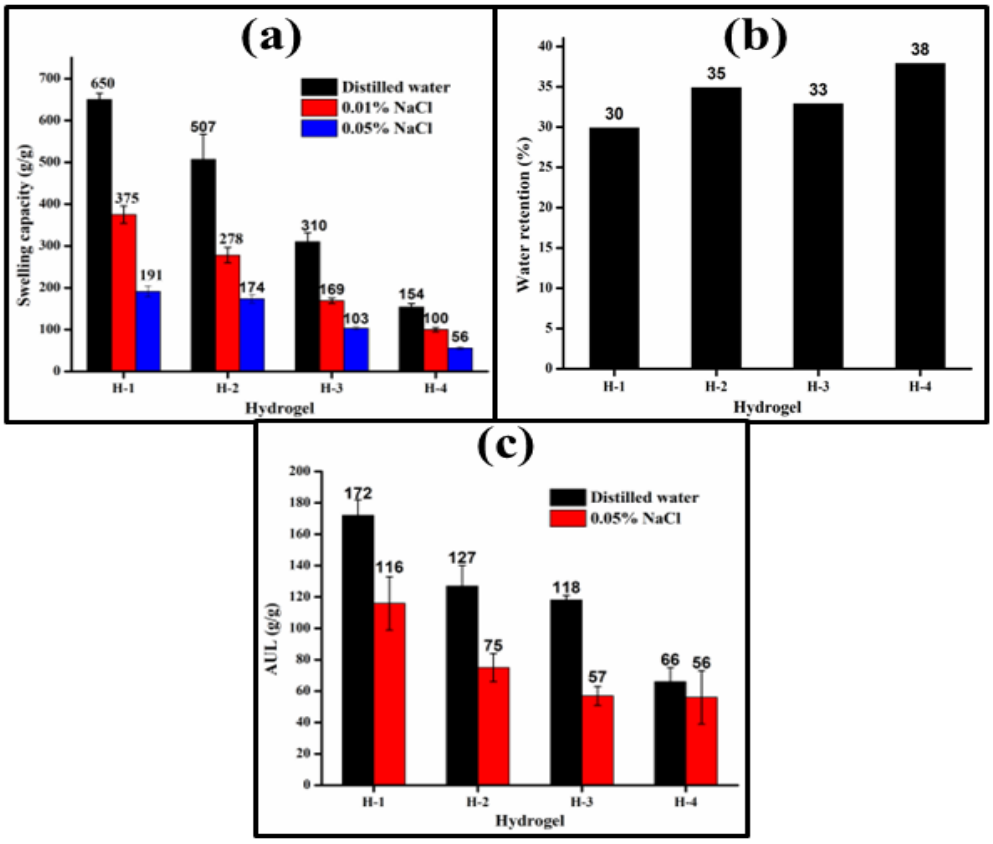

Figure 2.4. (a) Swelling capacity of hydrogels in different media, (b) water retention percentage in saline solution, and (c) water AUL.

2.3.2.5. Estimation of grafted IA and AA content in the SAHs

The quantity of IA and AA that grafted to the SAHs were determined from the results obtained from acid-base titration of unreacted material extracted from the SAH. The total number of moles of IA and AA present in the unreacted material extracted from H-2, H-3 and H-4 were found to be 5.4×10^{-5}, 6.3×10^{-5} and 9.9×10^{-5} mol, respectively which indicated that more than 99% of IA and AA from the initial reaction mixture get grafted to the SAHs. Thus, it was observed that with the increase in the amount of IA in the initial mixture increase the amount of IA grafted on the SAH backbone, indicating the presence of more -COOH groups in the hydrogel matrix. Therefore, the effect of IA in the SAHs can be ascribed to the decreasing nature of WAC and increasing behavior of

water retention capacity (in salt solution) of the SAHs which are already discussed in **Section 2.3.2.4**. Because the presence of unionized -COOH groups is responsible for increment of hydrophobic nature of hydrogel for which WAC of hydrogel decreases [32]. In the case of salt solution, presence of higher amount of -COOH group pronounced more the shielding effect of sodium cation on the carboxylate groups of IA and AA that increased the retention of water molecules within the hydrogel network structure.

2.3.2.6. AUL studies of the hydrogels

Water AUL is an important parameter that determines the strength of swollen SAHs. Therefore, it has been tried to get SAHs with higher water AUL values. In this work, water AUL values for synthesized SAHs were determined in water and saline solution and the obtained values are presented in **Figure 2.4.c**. The samples H-1, H-2, H-3 and H-4 exhibited water AUL of 172 g/g, 127 g/g, 118 g/g, and 66 g/g in water and 116 g/g, 75 g/g, 57 g/g, and 56 g/g in the salt solution, respectively. These results indicate that there is a similar decreasing trend, both in water AUL values and load-free absorbance. As shown in **Figure 2.4.c**, the water AUL value was found to decrease in both the media when the amount of IA was increased in the prepared SAH. This result may be responsible for decreasing trend of the degree of cross-linking present in the hydrogel network. It has been observed that an increase in cross-linking density enhances the water AUL value. This is because an increment in the cross-linker content leads to a further increase in the cross-linking density and hence the gel strength of the SAH. This in turn led to hold more water molecules tightly within the 3D structure even under certain loads [15,49].

2.3.2.7. Kinetic studies

2.3.2.7.1. Water diffusion of the hydrogels

To understand the water transport mechanism in agriculture, it is important to study the swelling kinetics of SAHs in different media [16]. The plots of log (W_t/W_{eq}) against log (t) for samples (H-1, H-2, H-3, and H-4) are shown in **Figure 2.5.a**. This figure shows that the obtained straight lines are linearly fitted with good correlation coefficients. The values of n and k which are obtained from the slope and intercept of the plotted lines, respectively and are tabulated in **Table 2.3**. The obtained n values for H-1, H-2, H-3 and H-4 are 0.0231, 0.0446, 0.0492, and 0.1198, respectively. Since all the samples exhibit n

values lower than 0.5, it indicates that the water transport mechanism of synthesized SAHs is a Fickian type diffusion in which water molecules diffuse simply through the pores of the hydrogel network structure [19]. Moreover, the n values were found to be increased from 0.0231 to 0.1198 with the increase in the amount of IA in the SAHs. This behavior can be attributed to the effect of IA on the GC of the SAHs. As provided in **Table 2.2**, after increasing the IA content from 0.1 to 0.3 g, GC was found to be decreased which in turn further lowered the gel strength of the SAHs. According to the literature report, pores between the cross-linked points become larger when gel strength decreases [12]. Therefore, it can be said that amount of IA that gets grafted on the backbone affected the porosity of the SAH. Thus, the increasing nature of n values may be attributed to the porous structure of the SAHs which further increased the contact surface area with water molecules and can be accounted for an increasing Fickian process.

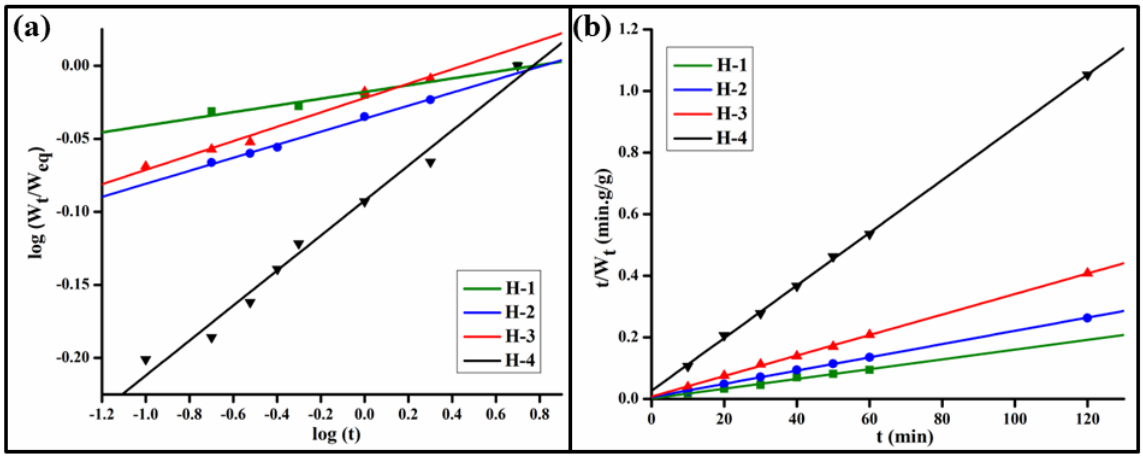

Figure 2.5. (a) Plots of log (W_t/W_{eq}) versus log t, and (b) plot of t/W_t versus t.

Table 2.3. Diffusion kinetic parameters of the hydrogels.

Hydrogel	Diffusion exponent (n)	Diffusion constant (k)	Correlation coefficient (R^2)
H-1	0.0231	0.9596	0.9393
H-2	0.0446	0.9200	0.9927
H-3	0.0492	0.9506	0.9771
H-4	0.1198	0.8086	0.9819

2.3.2.7.2. PSO kinetic study for the swelling

To get more information about swelling behavior, a PSO kinetic model was applied to study the swelling kinetics of the prepared SAHs. For this, a linear plot of (t/W_t) versus (t) was obtained for the hydrogels as shown in **Figure 2.5.b**. As clearly seen, the

obtained straight lines are found to be linearly fitted with a good linear correlation coefficient which confirmed that the PSO model can be effectively used to study the swelling kinetics of as prepared SAHs. The swelling kinetic parameters, W_{eq} and k_s are calculated from the slope and the intercept of the obtained straight lines, respectively and are provided in **Table 2.4**. The theoretically calculated W_{eq} values for H-1, H-2, H-3, and H-4 are 591 g/g, 465 g/g, 300 g/g, and 116 g/g, respectively, which are very close to the experimental equilibrium swelling values of the SAHs. Moreover, an increasing trend for k_s value was observed for H-2, H-3 and H-4 and the highest k_s value of 2.81×10^{-3} ($g.g^{-1}min^{-1}$) was obtained for H-4. These results suggested that H-4 exhibits the fastest water absorption rate as compared to the other SAHs due to the easy permeation of water molecules through the pores of the hydrogel. This can be attributed to a decrease in cross-linking density that results in increasing of space in the 3D structure which facilitates the easy diffusion of water molecules to the hydrogel network [26,33]. Therefore, an increasing behavior for water absorption rate was observed as shown in **Table 2.4**.

Table 2.4. Swelling kinetic parameters of H-1, H-2, H-3 and H-4 hydrogels.

Hydrogel	k_s ($g.g^{-1}min^{-1}$)	W_{eq} ($g.g^{-1}$)	Correlation coefficient (R^2)
H-1	1.81×10^{-3}	591	0.9873
H-2	0.79×10^{-3}	465	0.9994
H-3	1.44×10^{-3}	300	0.9992
H-4	2.81×10^{-3}	116	0.9995

2.3.2.8. Urea loading efficiency and release profile studies

Before performing urea release studies, loading efficiency for all the urea encapsulated hydrogels was determined. All these SAHs showed good urea loading efficiency. The observed loading efficiency for UH-1, UH-2, UH-3 and UH-4 were 93%, 92%, 94%, and 90%, respectively.

The urea release rate of the hydrogel mainly depends on the water absorbency and the cross-linking density of the hydrogel network [31]. A higher WAC leads to the diffusion of more water into the hydrogel network resulting in the release of a greater amount of urea molecules. Moreover, a highly cross-linked network can tightly hold urea molecules, as a result, they are slowly released from the hydrogel network. The urea release profiles of UH-1, UH-2, UH-3, and UH-4 for 30 days in distilled water are shown

in **Figure 2.6.a**. All the USAHs exhibited an increasing trend of urea release rate with exposure time. Initially, all the USAHs exhibited an increasing trend of urea release rate for the first 15 days. Then from 15 to 20 days, a significant increase in the release rate of urea was observed for UH-2, attributing to faster nitrogen release due to its more water absorption capacity, as high Q_{max} corresponds to quick nutrient release [31]. However, as compared to UH-2, UH-1 showed a lower released rate due to the higher strength of the hydrogel network that holds the urea molecules tightly within their network structure. It was also seen that with time, the strength of the hydrogels to hold the urea molecules decreases and almost 84% of the loaded urea was released within 30 days. The slowest release rate over 30 days was observed in the case of UH-4. This may be due to the formation of more cross-linking points into the hydrogel matrix (UH-4) [31]. This makes the hydrogel matrix to be stronger, and more rigid so that it can hold urea molecules more tightly. Only 35% of the encapsulated urea was released after 30 days. Therefore, UH-4 is considered to be the slowest urea released SAH among the four prepared USAHs.

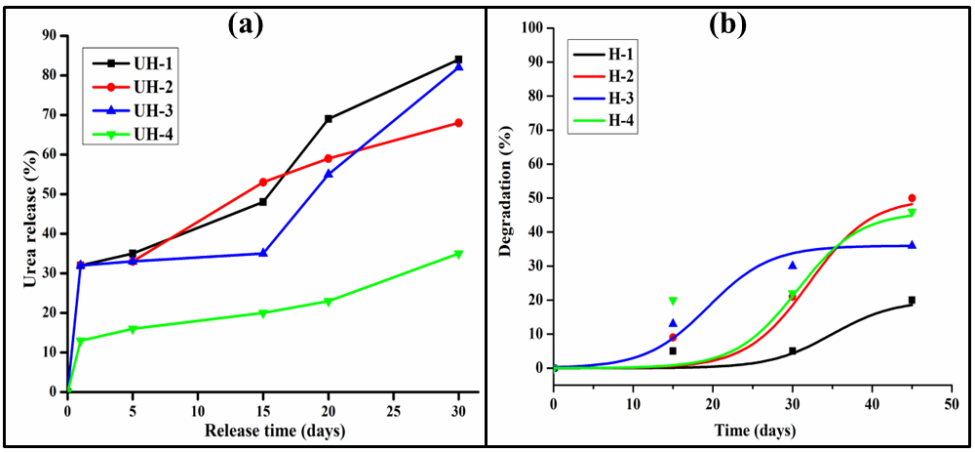

Figure 2.6. (a) Urea release profiles and (b) biodegradation percentage with exposure time of hydrogels.

2.3.2.9. Biodegradation study of the SAHs

Biodegradability is considered to be one of the most important properties of SAH for agricultural applications. SAHs are primarily utilized in agricultural applications and the retention of polymeric materials in soil for a longer period result in serious environmental pollution [13]. Therefore, the biodegradability of prepared hydrogels was observed. and their degradation percentages for 45 days are presented in **Figure 2.6.b**. From this figure, it is observed that all the hydrogels showed a gradual increase in biodegradation rate with the increasing length of soil burial time. This is because

different kinds of microorganisms are present in the soil that start to invade the hydrogel network after getting buried in the soil which subsequently leads to a decrease in the weight of the SAHs [13]. Initially, a rapid degradation rate was observed for H-4 for 15 days. It may be due to the presence of more biocomponents in H-4 that facilitate a rapid attack on the starch backbone by the microorganisms present in the soil [26]. However, the rate of degradation was found to decrease between 15 to 30 days. This can be attributed to the formation of an anaerobic environment due to an increase of water to mass ratio that inhibits the growth of microorganisms [26]. After 30 days, a rapid increase in the rate of degradation was observed for H-2 and H-4 due to the breaking down of hydrogel into smaller fragments that facilitate the microbial attack [12].

2.3.2.10. WHC of the soil

As shown in **Figure 2.7.a**, a measurable increase in WHC for soil treated with USAHs was observed as compared to the control. After 3 days, the percentages of WHC for the soil treated with UH-1, UH-2, UH-3 and UH-4 were found to be 45%, 41%, 39% and 37%, respectively. From these results, it was observed that the addition of 0.2% (w/w) of USAH, the WHC of the soil was improved which was significantly higher than the control soil (33%). This is because SAHs can retain the absorbed water for a long time and slowly release it into the soil [33]. Therefore, it can be said that the prepared SAHs can be used as an effective water reservoir for agricultural applications. Similarly, Thombare *et. al.* reported improved WHC of soil upon the addition of 0.1% of guar-gum-based hydrogel powder [26].

2.3.2.11. PD, BD and porosity of the soil

Using **Eq. 2.13**, the PD of the soil was determined which was found to be 2.53 g/cm^3. As shown in **Figure 2.7.b**, it is observed that there is a significant difference in BD between the treated and untreated soil. The obtained BD for the untreated soil was 0.96 g/cm^3, whereas soil treated with UH-1, UH-2, UH-3 and UH-4 were found to be 0.62, 0.67, 0.74 and 0.76 g/cm^3, respectively. It has been reported that the addition of hydrogel facilitates the formation of macropores in the soil for which BD of the treated soil becomes lower as compared to the untreated soil [27]. This happens because when hydrogel particles are dehydrated from their swollen state, they leave voids between the soil particles [26]. However, a linearly increasing trend in BD was observed for the treated soil. The soil

treated with UH-1 exhibited the lowest BD and the highest value was noticed for soil treated with UH-4. This behavior can be attributed to their respective WHC of soil.

Based on PD and BD, porosity values of the treated and untreated soil were calculated, and the results are shown in **Figure 2.7.c**. Soil treated with UH-1, UH-2, UH-3 and UH-4 showed porosities of 75.5%, 73.3%, 70.6%, and 70%, respectively, as compared to 62.1% of the control. From these results, it was observed that the porosity of the soil increases with the decrease in BD value. This is because the lower density defines a greater volume for the same weight [26]. Therefore, from the lower BD and higher porosity of treated soil, it can be said that prepared USAH can provide good health to the soil by increasing oxygen as well as fertilizer supplies along with water and can be used for the plant growth.

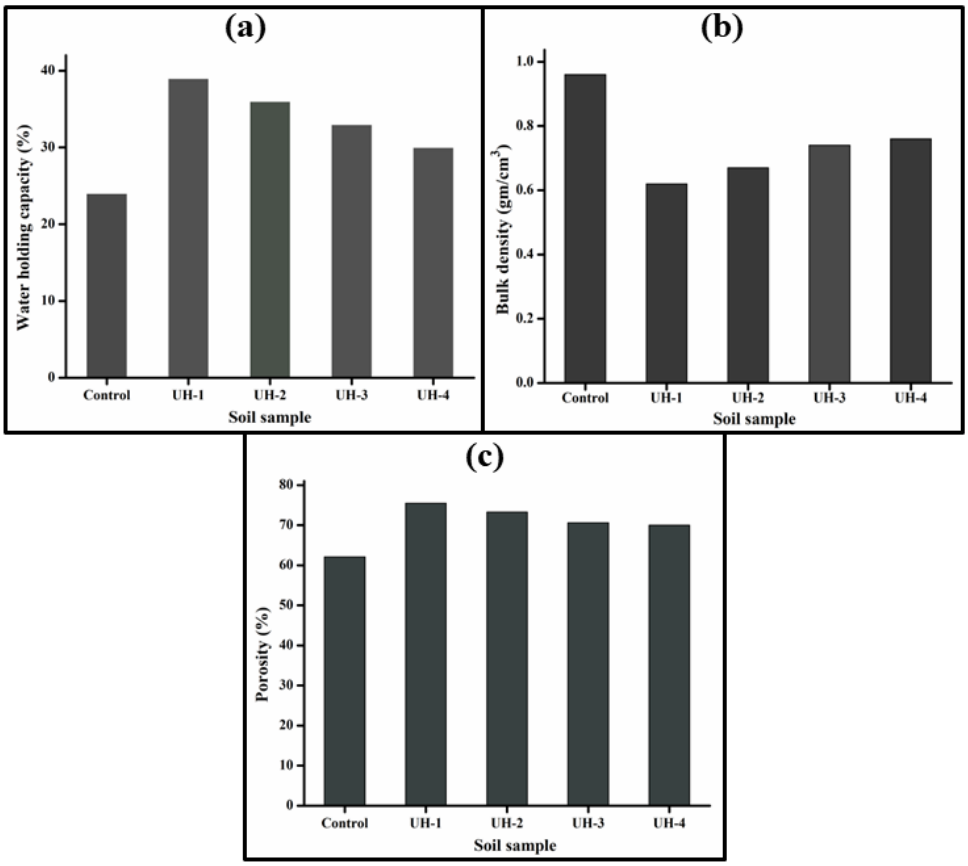

Figure 2.7. Effect of urea loaded SAHs on (a) WHC, (b) BD and (c) porosity of soil.

2.3.2.12. Seed germination rate

The germination rate of okra seeds in all the soil media was recorded after 7 days of sowing and was calculated by using **Eq. 2.16**. The rate of germination for UH-1, UH-2, UH-3, UH-4, control-1 and control-2 was found to be 67%, 78%, 67%, 56%, 44% and 33%, respectively. Under no water irrigation conditions, seed germination in the

presence of USAH, showed a higher germination rate as compared to the control, as shown in **Figure 2.8**. This is because the presence of SAHs gradually supplies, even in absence of irrigation, a certain amount of water to the seeds [28]. This can also be confirmed from the comparison of germination rate between control-1 and control-2. In the case of control-1, the presence of SAHs facilitate water for germination, while there was no such facility in the case of control-2 which led to a germination rate of only 33%. Higher seed germination rate obtained for soils with urea treated SAH compared to untreated soil can be ascribed to their higher Q_{max} value that might facilitate a moist environment as well as loaded fertilizer for seed germination [34]. From **Figure 2.8**, the highest germination rate was obtained for UH-2, even though UH-1 exhibited the highest Q_{max} value. This result may be due to the fact that at this composition, the used soil media is most suitable for germination of okra seeds. Thus, it can be concluded that the rate of germination of okra seeds can be enhanced by applying the appropriate USAHs.

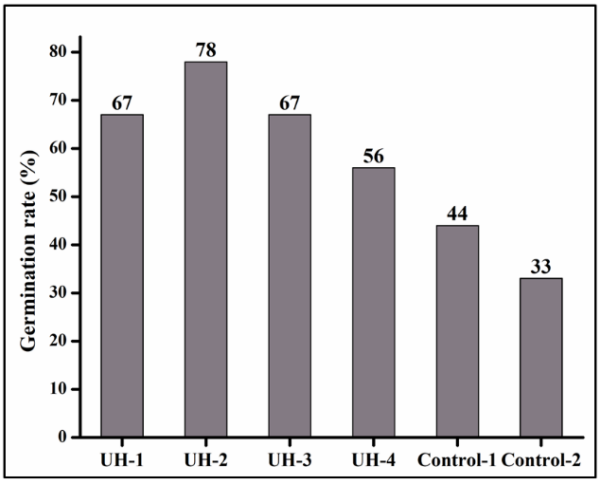

Figure 2.8. Seed germination rate under different media.

2.4. Conclusion

In this work, four SAHs were successfully prepared by grafting AA and IA on the starch backbone with MBA cross-linker. The formation of a 3D cross-linked network structure of prepared SAHs was supported by FTIR and SEM studies. The synthesized SAHs showed decreasing water swelling values with an increase in the percentage of biocomponent for all the three swelling media but high water retention values. The percentage of water retention was found to be 38% for H-4 compared to 30% for H-1, when the percentage of biocomponent was increased from 48% to 63%. The water AUL values were found to be consistent with the percentage of GC of the prepared SAHs. All the samples follow the water transport mechanism according to Fickian type diffusion.

Further, the study of the PSO kinetic model indicates that the theoretical water swelling values are close to the experimental values and the highest swelling rate constant is obtained for H-4. In the case of urea loading efficiency, all four-hydrogels showed more than 90% loading capacity and it was found that UH-4 possesses more slow-release behavior as well as a faster biodegradation rate. Moreover, the addition of 0.2 wt% of prepared USAHs enhanced the WHC and porosity of the soil and a significantly higher seed germination rate was also observed for the treated soil than in the untreated one.

References

[1] Choi, H., Park, J., and Lee, J. Sustainable bio-based superabsorbent polymer: Poly(itaconic acid) with superior swelling properties. *ACS Applied Polymer Materials*, 4(6):4098-4108, 2022.

[2] Hakim, S., Darounkola, M. R. R., HaniehTalari, Barghemadi, M., and Parvazinia, M. Fabrication of PVA/nanoclay hydrogel nanocomposites and their microstructural effect on the release behavior of a potassium phosphate fertilizer. *Journal of Polymers and the Environment*, 27:2925-2932, 2019.

[3] Yang, J., Han, C. R., Duan, J. F., Ma, M. G., Zhang, X. M., Xu, F., Sun, R. C., and Xie, X. M. Studies on the properties and formation mechanism of flexible nanocomposite hydrogels from cellulose nanocrystals and poly(acrylic acid). *Journal of Materials Chemistry*, 22(42):22467-22480, 2012.

[4] Li, D., Gao, H., Li, M., Chen, G., Guan, L., He, M., Tian, J., and Cao, R. Nanochitin/metal ion dual reinforcement in synthetic poly(acrylamide) network-based nanocomposite hydrogels. *Carbohydrate Polymers*, 236:116061, 2020.

[5] Dhanapal, V., Subhapriya, P., Nithyanandam, K. P., Kiruthika, M. V., Keerthana, T., and Dineshkumar, G. Design, synthesis and evaluation of N,N'-methylene bis-acrylamide crosslinked smart polymer hydrogel for the controlled release of water and plant nutrients in agriculture field. *Materials Today: Proceedings*, 45:2491-2497, 2021.

[6] Liu, T. G., Wang, Y. T., Guo, J., Liu, T. B., Wang, X., and Li, B. One-step synthesis of corn starch urea-based acrylate superabsorbents. *Journal of Applied Polymer Science*, 134(32):45175, 2017.

[7] Pourjavadi, A., Harzandi, A. M., and Hosseinzadeh, H. J. E. P. J. Modified carrageenan 3. Synthesis of a novel polysaccharide-based superabsorbent

hydrogel via graft copolymerization of acrylic acid onto kappa-carrageenan in air. *European Polymer Journal*, 40(7):1363-1370, 2004.

[8] Dan, S., Banivaheb, S., Hashemipour, H., and Kalantari, M. Synthesis, characterization and absorption study of chitosan-g-poly(acrylamide-co-itaconic acid) hydrogel. *Polymer Bulletin*, 78:1887-1907, 2021.

[9] Demitri, C., Del Sole, R., Scalera, F., Sannino, A., Vasapollo, G., Maffezzoli, A., Ambrosio, L., and Nicolais, L. Novel superabsorbent cellulose-based hydrogels crosslinked with citric acid. *Journal of Applied Polymer Science*, 110(4):2453-2460, 2008.

[10] Durpekova, S., Bergerova, E. D., Hanusova, D., Dusankova, M., and Sedlarik, V. Eco-friendly whey/polysaccharide-based hydrogel with poly(lactic acid) for improvement of agricultural soil quality and plant growth. *International Journal of Biological Macromolecules*, 212:85-96, 2022.

[11] Birajdar, M. S., Joo, H., Koh, W. G. and Park, H. Natural bio-based monomers for biomedical applications: A review. *Biomaterials Research*, 25(1):1-14, 2021.

[12] Sarmah, D. and Karak, N. Biodegradable superabsorbent hydrogel for water holding in soil and controlled-release fertilizer. *Journal of Applied Polymer Science*, 137(13):48495, 2020.

[13] Mohammadbagheri, Z., Rahmati, A., and Hoshyarmanesh, P. Synthesis of a novel superabsorbent with slow-release urea fertilizer using modified cellulose as a grafting agent and flexible copolymer. *International Journal of Biological Macromolecules*, 182:1893-1905, 2021.

[14] Kyzas, G. Z., Siafaka, P. I., Lambropoulou, D. A., Lazaridis, N. K., and Bikiaris, D. N. Poly(itaconic acid)-grafted chitosan adsorbents with different cross-linking for Pb (II) and Cd (II) uptake. *Langmuir*, 30(1):120-131, 2014.

[15] Kim, H. C., Kwon, Y. R., Kim, J. S., Kim, J. H., and Kim, D. H. Novel itaconic acid-based superabsorbent polymer composites using oxidized starch. *Polymer-Plastics Technology and Materials*, 61(4):374-383, 2022.

[16] Bueno, V. B., Bentini, R., Catalani, L. H., and Petri, D. F. S. Synthesis and swelling behavior of xanthan-based hydrogels. *Carbohydrate Polymers*, 92(2):1091-1099, 2013.

[17] Yiamsawas, D., Kangwansupamonkon, W., Chailapakul, O., and Kiatkamjornwong, S. Synthesis and swelling properties of poly[acrylamide-co-

(crotonic acid)] superabsorbents. *Reactive and Functional Polymers*, 67(10):865-882, 2007.

[18] Zonatto, F., Muniz, E. C., Tambourgi, E. B., and Paulino, A. T. Adsorption and controlled release of potassium, phosphate and ammonia from modified arabic gum-based hydrogel. *International Journal of Biological Macromolecules*, 105:363-369, 2017.

[19] Gharekhani, H., Olad, A., Mirmohseni, A., and Bybordi, A. Superabsorbent hydrogel made of NaAlg-g-poly(AA-co-AAm) and rice husk ash: Synthesis, characterization, and swelling kinetic studies. *Carbohydrate Polymers*, 168:1-13, 2017.

[20] Olad, A., Doustdar, F., and Gharekhani, H. Starch-based semi-IPN hydrogel nanocomposite integrated with clinoptilolite: Preparation and swelling kinetic study. *Carbohydrate Polymers*, 200:516-528, 2018.

[21] Giraldo, J. D. and Rivas, B. L. Determination of urea using 4-(dimethylamino)benzaldehyde: Solvent effect and interference of chitosan. *Journal of the Chilean Chemical Society*, 62(2):3538-3542, 2017.

[22] Dutta, G. K. and Karak, N. One-pot synthesis of bio-based waterborne polyester as UV-resistant biodegradable sustainable material with controlled release attributes. *ACS Omega*, 3(12):16812-16822, 2018.

[23] Dutta, S., Karak, N., Saikia, J. P., and Konwar, B. K. Biodegradation of epoxy and MF modified polyurethane films derived from a sustainable resource. *Journal of Polymers and the Environment*, 18:167-176, 2010.

[24] Saruchi, Kaith, B. S., Jindal, R., and Kapur, G. S. Enzyme-based green approach for the synthesis of gum tragacanth and acrylic acid cross-linked hydrogel: Its utilization in controlled fertilizer release and enhancement of water-holding capacity of soil. *Iranian Polymer Journal*, 22:561-570, 2013.

[25] Blake, G. R. Particle density. In Black, C. A., Evans, D. D., White, J. L., Ensminger, L. E., and Clark, F E., editors, *Methods of soil analysis. Part 1. Physical and mineralogical properties, including statistics of measurement and sampling*, Pages 374-390. American Society of Agronomy, 1965.

[26] Thombare, N., Mishra, S., Siddiqui, M. Z., Jha, U., Singh, D., and Mahajan, G. R. Design and development of guar gum-based novel, superabsorbent and moisture retaining hydrogels for agricultural applications. *Carbohydrate Polymers*, 185:169-178, 2018.

[27] Nascimento, C. D. V., Mota, J. C. A., Nascimento, Í. V., da Silva Albuquerque, G. H., Simmons, R. W., dos Santos Dias, C. T., and Costa, M. C. G. Temperature limitations in the use of hydrogels on leptosols in a semi-arid region of Brazil. *Geoderma Regional*, 26:e00407, 2021.

[28] Montesano, F. F., Parente, A., Santamaria, P., Sannino, A., and Serio, F. Biodegradable superabsorbent hydrogel increases water retention properties of growing media and plant growth. *Agriculture and Agricultural Science Procedia*, 4:451-458, 2015.

[29] Zhu, J., Tan, W. K., Song, X., Gao, Z., Wen, Y., Ong, C. N., Loh, C. S., Swarup, S., and Li, J. Converting okara to superabsorbent hydrogels as soil supplements for enhancing the growth of choy sum (*Brassica sp.*) under water-limited conditions. *ACS Sustainable Chemistry and Engineering*, 8(25):9425-9433, 2020.

[30] Liu, T. G., Wang, Y. T., Li, B., Deng, H. B., Huang, Z. L., Qian, L. W., and Wang, X. Urea free synthesis of chitin-based acrylate superabsorbent polymers under homogeneous conditions: Effects of the degree of deacetylation and the molecular weight. *Carbohydrate Polymers*, 174:464-473, 2017.

[31] Salimi, M., Motamedi, E., Motesharezedeh, B., Hosseini, H. M., and Alikhani, H. A. Starch-g-poly(acrylic acid-co-acrylamide) composites reinforced with natural char nanoparticles toward environmentally benign slow-release urea fertilizers. *Journal of Environmental Chemical Engineering*, 8(3):103765, 2020.

[32] Pulat, M. and Eksi, H. Determination of swelling behavior and morphological properties of poly(acrylamide-co-itaconic acid) and poly(acrylic acid-co-itaconic acid) copolymeric hydrogels. *Journal of Applied Polymer Science*, 102(6):5994-5999, 2006.

[33] Motamedi, E., Motesharezedeh, B., Shirinfekr, A., and Samar, S. M. Synthesis and swelling behavior of environmentally friendly starch-based superabsorbent hydrogels reinforced with natural char nano/micro particles. *Journal of Environmental Chemical Engineering*, 8(1):103583, 2020.

[34] Tang, H., Zhang, L., Hu, L., and Zhang, L. Application of chitin hydrogels for seed germination, seedling growth of rapeseed. *Journal of Plant Growth Regulation*, 33:195-201, 2014.